

# Pollution events over the East Mediterranean: Synergistic use of GOME, ground-based and sonde observations and models

A. Ladstätter-Weißenmayer<sup>a,\*</sup>, M. Kanakidou<sup>b</sup>, J. Meyer-Arnek<sup>c</sup>, E.V. Dermitzaki<sup>b</sup>,  
A. Richter<sup>a</sup>, M. Vrekoussis<sup>a,b</sup>, F. Wittrock<sup>a</sup>, J.P. Burrows<sup>a</sup>

<sup>a</sup>*Institute of Environmental Physics, University of Bremen, P.O. Box 330440, D-28334 Bremen, Germany*

<sup>b</sup>*Environmental Chemical Processes Laboratory, Department of Chemistry, University of Crete, P.O. Box 2208, GR-71003 Heraklion, Greece*

<sup>c</sup>*German Aerospace Center (DLR), German Remote Sensing Data Center (DFD), Oberpfaffenhofen, D-82234 Wessling, Germany*

Received 1 September 2006; received in revised form 7 May 2007; accepted 14 May 2007

## Abstract

The behaviour of ozone ( $O_3$ ) and two important precursors, nitrogen dioxide ( $NO_2$ ) and formaldehyde (HCHO), over the East Mediterranean in spring from 1996 to 2002 is studied in order to characterise the buildup of tropospheric  $O_3$ . The vertical distribution of  $O_3$  observed over Crete during the Photochemical Activity and Solar Ultraviolet Radiation (PAUR II) campaign in May 1999 has been used for validation of satellite-derived data. Retrievals of  $O_3$  columns from measurements of backscattered radiation by Global Ozone Monitoring Experiment (GOME) are compared with Total Ozone Mapping Spectrometer (TOMS), balloon, Systeme d'Analyse par Observation Zenithale (SAOZ) and LIDAR observations. The total  $O_3$  vertical columns vary between 270 and 402 DU and correlate well with changes in air circulation patterns. The total observed variability in tropospheric  $O_3$  is about 25 DU. Chemical box model calculations associate the GOME-observed  $NO_2$  and HCHO tropospheric columns with a potential of daily photochemical enhancement in the tropospheric  $O_3$  columns of about 0.8–1 DU over Crete and estimate the daily potential of regional photochemical buildup within upwind polluted air masses at about 2–8 DU. A Langrangian analysis attributes at most 10–20 DU of tropospheric  $O_3$  to stratosphere–troposphere exchange (STE). The remainder is attributed to long-range transport of  $O_3$  from industrial regions in Central Europe. From 1996 to 2002, in May no significant inter-annual variation in the tropospheric  $NO_2$  and HCHO columns over Crete has been observed by GOME suggesting no detectable increase in regionally produced tropospheric  $O_3$ .

© 2007 Elsevier Ltd. All rights reserved.

**Keywords:** Pollution; East Mediterranean; GOME; Ground-based measurements; Sonde observations; Model output

## 1. Introduction

The troposphere over the Mediterranean is influenced by air masses transported from surrounding and distant areas (e.g., Central Europe

and/or the Balkans) as well as from the stratosphere above. This leads to variations in its composition. Elevated amounts of the ozone ( $O_3$ ) precursors nitrogen dioxide ( $NO_2$ ) and formaldehyde (HCHO) are indicators of polluted air masses (Fishman and Crutzen, 1978). In addition, HCHO is formed by the oxidation of biogenic volatile organic compounds (VOCs) (Wayne, 2000) emitted in the areas surrounding the Mediterranean. The mixing with

\*Corresponding author.

E-mail address: [lad@iup.physik.uni-bremen.de](mailto:lad@iup.physik.uni-bremen.de)  
(A. Ladstätter-Weißenmayer).

anthropogenic emissions of nitrogen oxides ( $\text{NO}_x$ ) and VOCs under the typically elevated photochemistry conditions in this area strongly favours the regional buildup of pollutants.

The transport of  $\text{NO}_2$ , HCHO and of  $\text{O}_3$  itself over hundreds or even thousands of kilometres is enabled by the sufficiently long lifetimes of these compounds (global mean lifetimes:  $\tau_{\text{NO}_2} = 1\text{--}2$  days,  $\tau_{\text{HCHO}} =$  a few hours,  $\tau_{\text{O}_3} = 1\text{--}3$  months) (Oltmans et al., 1998; Lawrence et al., 2006). The present study focuses on the changes in tropospheric  $\text{O}_3$ ,  $\text{NO}_2$  and HCHO during May from 1996 to 2002 and particularly in the year 1999 when the Photochemical Activity and Solar Ultraviolet Radiation (PAUR II) experiment took place over Crete located in the South East Mediterranean (Zerefos et al., 2002).

The analysis makes synergistic use of remotely sensed and in situ data including satellite-based observations by Global Ozone Monitoring Experiment (GOME) (Burrows et al., 1999) and Total Ozone Mapping Spectrometer (TOMS), measurements (Hudson and Thompson, 1998) from balloon and ground-based LIDAR and Systeme d'Analyse par Observation Zenithale (SAOZ) instruments (Goutail and Pommereau, 1991; Goutail et al., 1999), back-trajectory analyses, as well as chemistry/transport and chemical box model calculations. After explaining the applied methods (Section 2), the usability of GOME data over Crete is shown by comparing total columns of  $\text{O}_3$  with SAOZ and TOMS data (Section 3.1). Then, different influences (transport and photochemical production) on tropospheric  $\text{O}_3$  levels are assessed by use of GOME, TOMS, sonde and LIDAR measurements as well as model results (Section 3.2). Finally, starting this detailed analysis for the month of May 1999 (Section 3.3), inter-annual and seasonal trends of  $\text{O}_3$  precursors including the impact of wind direction are presented (Section 3.4).

In particular, the photochemical formation of  $\text{O}_3$  was evaluated by chemical box model simulations, whereas the irreversible mixing of ozone-rich stratospheric air masses into the troposphere, stratosphere–troposphere exchanges (STE) and the general long-range transport of air masses were addressed by trajectory analyses.

## 2. Methods

### 2.1. GOME

GOME was launched in April 1995 onboard the second European satellite ERS-2 in a sun-synchro-

nous near-polar orbit at a mean altitude of 795 km crossing the equator at 10:30 a.m. local time. The instrument measures sunlight back-scattered from Earth's atmosphere or reflected by the surface in nadir mode in a wavelength region of 240–790 nm with a spectral resolution of 0.2–0.4 nm and a ground pixel size of  $40 \times 320 \text{ km}^2$ . With 14 orbits per day, global coverage at the equator is reached after 3 days for a 960 km swath width (Burrows et al., 1999).

For this study, GOME data were reprocessed with weighting function differential optical absorption spectroscopy (WFDOAS) Version 1 (Coldey-Egbers et al., 2005; Weber et al., 2005) to derive vertical columns of  $\text{O}_3$  with an uncertainty of 3%. The retrieval of slant columns of  $\text{NO}_2$  in the wavelength region of 425–450 nm (Burrows et al., 1999; Richter and Burrows, 2002) and of HCHO between 337.5 and 359 nm (Ladstätter-Weißmayer et al., 1998; Chance et al., 2000; Palmer et al., 2002) were accomplished using the IUP Bremen DOAS algorithm. The slant column density (SCD) is the amount of the absorber along the total light path through the atmosphere. The SCD is converted to a total vertical column density ( $\text{VCD}_{\text{tot}}$ ), the vertically integrated absorber concentration, by using the so-called air mass factor (AMF) (Rozanov et al., 1997). The AMF is determined via radiative transfer calculations including information about aerosol, surface albedo and vertical absorber profile. In the following, a given column value always refers to the VCD.

GOME observes both, the troposphere and the stratosphere (Burrows et al., 1999). In cloudy conditions, the detection of trace gases below the cloud layer is impossible. For the retrieval of the tropospheric column amounts, only GOME pixels under cloud-free conditions with a cloud fraction  $< 0.2$  as determined by the FRESCO algorithm (Koelemeijer et al., 2001) were included.

The tropospheric trace gas column densities ( $\text{VCD}_{\text{trop}}$ ) were derived by applying the tropospheric excess method (TEM, also called reference sector approach). The TEM is based on the assumption that the stratospheric column of trace gases such as  $\text{NO}_2$  and  $\text{O}_3$  is approximately constant with longitude (Richter and Burrows, 2002; Chance et al., 2000; Fishman et al., 1990; Leue et al., 2001). This simplification works well for tropical and subtropical conditions for  $\text{O}_3$  and  $\text{NO}_2$  and for  $\text{NO}_2$  also for higher latitudes.

Several studies have been published focusing on the retrieval of tropospheric  $\text{NO}_2$  (Leue et al., 2001;

Richter and Burrows, 2002; Martin et al., 2002) and O<sub>3</sub> (Ladstätter-Weissenmayer et al., 2004) from GOME data. The tropospheric background amount at the reference sector in the Pacific region (180°E/W) and the accuracy of the resulting tropospheric amount for a single measurement are estimated to 25 DU (Dobson Units, 1 DU = 2.69 × 10<sup>16</sup> molecules cm<sup>-2</sup>) and 4 DU, respectively, for O<sub>3</sub> (Ladstätter-Weissenmayer et al., 2004) and approximately 1.5 × 10<sup>15</sup> and 2.5 × 10<sup>14</sup> molecules cm<sup>-2</sup> for NO<sub>2</sub>, respectively (Boersma et al., 2004; Richter and Burrows, 2002). In contrast to O<sub>3</sub> and NO<sub>2</sub>, HCHO is mainly located in the troposphere. Therefore, for a single measurement the tropospheric amount of HCHO can be determined directly with an accuracy of 5.0 × 10<sup>15</sup> molecules cm<sup>-2</sup>.

## 2.2. The chemical box model

The potential of photochemical ozone formation ( $P_{O_3}$ , in terms of DU day<sup>-1</sup>) from NO<sub>2</sub> and HCHO tropospheric columns observed over polluted areas upwind the Mediterranean region has been investigated by using a chemical box model. This well established chemical box model has been already applied to simulate the impact of VOCs on O<sub>3</sub>, OH and RO<sub>2</sub> radicals in forested areas (Poisson et al., 2001; Tsigaridis and Kanakidou, 2002) as well as the chemistry of NO<sub>x</sub> in the marine boundary layer of the East Mediterranean (Vrekoussis et al., 2004, 2006). The model uses the latest knowledge on chemical reactions and reaction rates (Atkinson et al., 2004, 2006). Seasonal and hourly mean values of CO, J(NO<sub>2</sub>) and J(O<sup>1</sup>D) observed over Crete are used as model input. Isoprene, ethene, propene, ethane, propane and butane mixing ratios are based on measurements performed in the area during an

8-month period (Liakakou et al., 2007). For this study, the model has been initialised by the GOME observations of NO<sub>2</sub> and HCHO over locations, mainly upwind Crete, as listed in Table 1. The columns have been translated to equivalent concentrations for a mean boundary layer height of 1.3 km as observed over Crete in spring, by Zerefos et al. (2002), by assuming that the trace compound mass lies entirely in the boundary layer. This simplified approach fails to simulate changes in the O<sub>3</sub> amount due to the oxidation of VOCs other than HCHO at levels above the regional background. In addition, the results are subject to boundary layer height uncertainties.

## 2.3. Back-trajectory analyses

Stratosphere–troposphere exchange plays an important role in the ozone budget of unpolluted regimes in the extratropics (Vaugh and Polvani, 2000; Randriambelo et al., 1999) and is characterised by the irreversible mixing of stratospheric air masses into the troposphere. To qualitatively and quantitatively assess STE over Crete, a back-trajectory analysis using Traj.x, the IUP Bremen trajectory model (Meyer-Arnek et al., 2005), has been carried out. ERA-40 data from the European Centre for Medium Range Weather Forecasts (ECMWF) are used as meteorological input. Clusters of back-trajectories are released over Crete at 0, 6, 12 and 18 h each day of May 1999 at altitudes between 900 and 100 hPa and are followed backwards in time for 5 days. The back-trajectories arriving in the troposphere and being influenced by the stratosphere at least once during the recent 5 days are considered to have undergone STE. The tropopause is defined here as the lowermost altitude

Table 1

Mean NO<sub>2</sub> and HCHO tropospheric column densities (molecules cm<sup>-2</sup>) and the corresponding HCHO/NO<sub>2</sub> ratio based on GOME data as well as the photochemical O<sub>3</sub> production (DU day<sup>-1</sup>) with and without VOCs impact for different regions (used grid boxes given in parenthesis) for May (1996–2002)

Trace gas	Atlantic (6–22°N; 27–40°W)	Crete (34–36°N; 24–26°E)	Athens (36–38°N; 21–24°E)	Thessaloniki (37–39°N; 22–27°E)	Istanbul (39–42°N; 27–32°E)	Po Valley (42–45°N; 7–14°E)
NO <sub>2</sub>	≤ 6.0 × 10 <sup>14</sup>	1.1 × 10 <sup>15</sup>	2.0 × 10 <sup>15</sup>	2.3 × 10 <sup>15</sup>	2.4 × 10 <sup>15</sup>	4.4 × 10 <sup>15</sup>
HCHO	3.1 × 10 <sup>15</sup>	4.7 × 10 <sup>15</sup>	4.9 × 10 <sup>15</sup>	4.6 × 10 <sup>15</sup>	4.5 × 10 <sup>15</sup>	6.6 × 10 <sup>15</sup>
HCHO/NO <sub>2</sub>	> 5.2	4.3	2.6	2.0	1.9	1.5
$P_{O_3}$	< 0.3	0.8–1.0 <sup>a</sup>	1.1–1.3	1.4–1.8	1.4–1.8	1.4–2.1
$P_{O_3\_VOC}$	0.0–1.2	<sup>a</sup>	2.1–3.9	2.6–5.2	2.6–5.2	3.6–7.9

The given ranges reflect uncertainties in the boundary layer height.

<sup>a</sup>For Crete, VOC observations have been used to initialise the model.

where either the potential vorticity (PV) exceeds  $\pm 3.5$  PV units (PVU) or the potential temperature exceeds 380 K.

Irreversible transport of air masses from the stratosphere to the troposphere and constant ozone content (number of molecules) in each considered air parcel crossing the tropopause are assumed. Maintaining the number of ozone molecules implies that the volume of the considered air parcel is adjusted to the current thermodynamical conditions. This method allows an estimate of the ozone mass being transported from the stratosphere to the troposphere and is subject to the uncertainties associated with the back-trajectories calculations discussed by Stohl et al. (2002). Neglecting chemical conversion of  $O_3$ , this approach overestimates stratospheric ozone transported to the troposphere.

The altitude-dependent stratospheric  $O_3$  number density for each considered air parcel crossing the tropopause is derived from the ROSE/DLR 3D CTM (Rose and Brasseur, 1989; Baier et al., 2005) that assimilates  $O_3$  column densities derived from GOME measurements by the means of optimal interpolation.

### 3. Results and discussion

#### 3.1. Total columns of $O_3$

To provide deeper understanding and to facilitate the interpretation of the tropospheric  $O_3$  retrieval discussed in the following section, amounts and changes in  $VCD_{tot} O_3$  in the East Mediterranean measured by GOME, TOMS and SAOZ in May 1999 have been investigated.

$O_3$   $VCD_{tot}$  over Crete retrieved from GOME measurements agree within 2.2% with TOMS data (McPeters, 1996) and within 3–4% with the SAOZ observations (Fig. 1). Both differences are smaller than the combined measurement errors of 5%. This comparison of  $VCD_{tot} O_3$  from GOME provides confidence to the satellite results.

The observed  $VCD_{tot} O_3$  exhibits strong fluctuations between 270 and 402 DU. Low values of 270 and 287 DU were observed during the periods of 1–5 and 15–23 May, respectively, and maximum values during 6–14 May (402 DU) and 24–31 May (360 DU). This high variability in  $VCD_{tot} O_3$  is associated with changes in atmospheric circulation as demonstrated by back-trajectory analyses (Fig. 2). The atmospheric regime over Crete, located in the sub-tropical region, changes frequently from

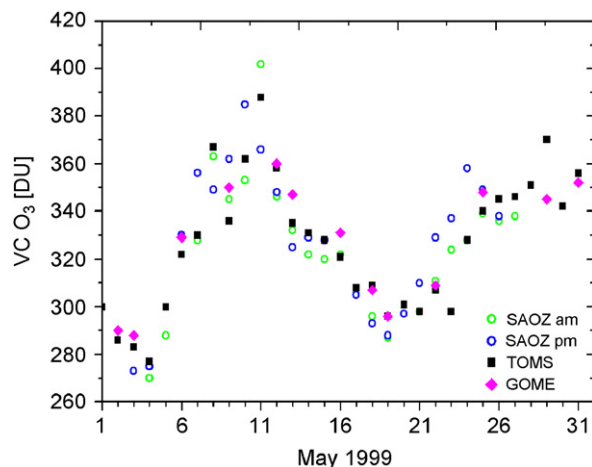


Fig. 1.  $VCD_{tot} O_3$  (DU) over Crete measured by GOME, compared to measurements by TOMS and SAOZ for May 1999.

a tropical to a mid-latitude regime. Therefore,  $VCD_{tot} O_3$  of around 270–290 DU are observed when air masses are transported from the tropics, whereas high  $O_3$  columns of up to 402 DU occur when air is coming from mid-latitudes. Such variations in  $VCD_{tot} O_3$  over regions located at the boundary of tropics and mid-latitudes has been attributed to changes in the location of the sub-tropical front (Hudson et al., 2003). Since each regime has a unique tropopause height (Hudson et al., 2003), we expect a changing tropopause height over this area. Indeed, the tropopause height, based on the 3.5 PVU criterion, is anti-correlated with the  $VCD_{tot} O_3$  (Fig. 3), which is not expected to be perfect since additional parameters (e.g., ozone chemistry) contribute to the observed total ozone.

#### 3.2. Tropospheric column of $O_3$

We further investigate the potential of GOME satellite observations to determine the influence of pollution events on tropospheric  $O_3$ ,  $NO_2$  and HCHO. During the MINOS (Mediterranean Intensive Oxidant Study) campaign in the East Mediterranean in 2001, GOME measurements yielded accurate tropospheric columns of  $NO_2$  and HCHO with levels close to the detection limit (Ladstätter-Weissenmayer et al., 2003). Hereafter,  $VCD_{trop}$  are evaluated for spring, a transition period with expected large variability in  $VCD_{tot} O_3$  as described above. For this purpose, the data from TOMS, LIDAR (Simeonov et al., 1998; Calpini et al., 1997) and ozonesonde (Thompson et al., 2003) measurements over Crete are used and

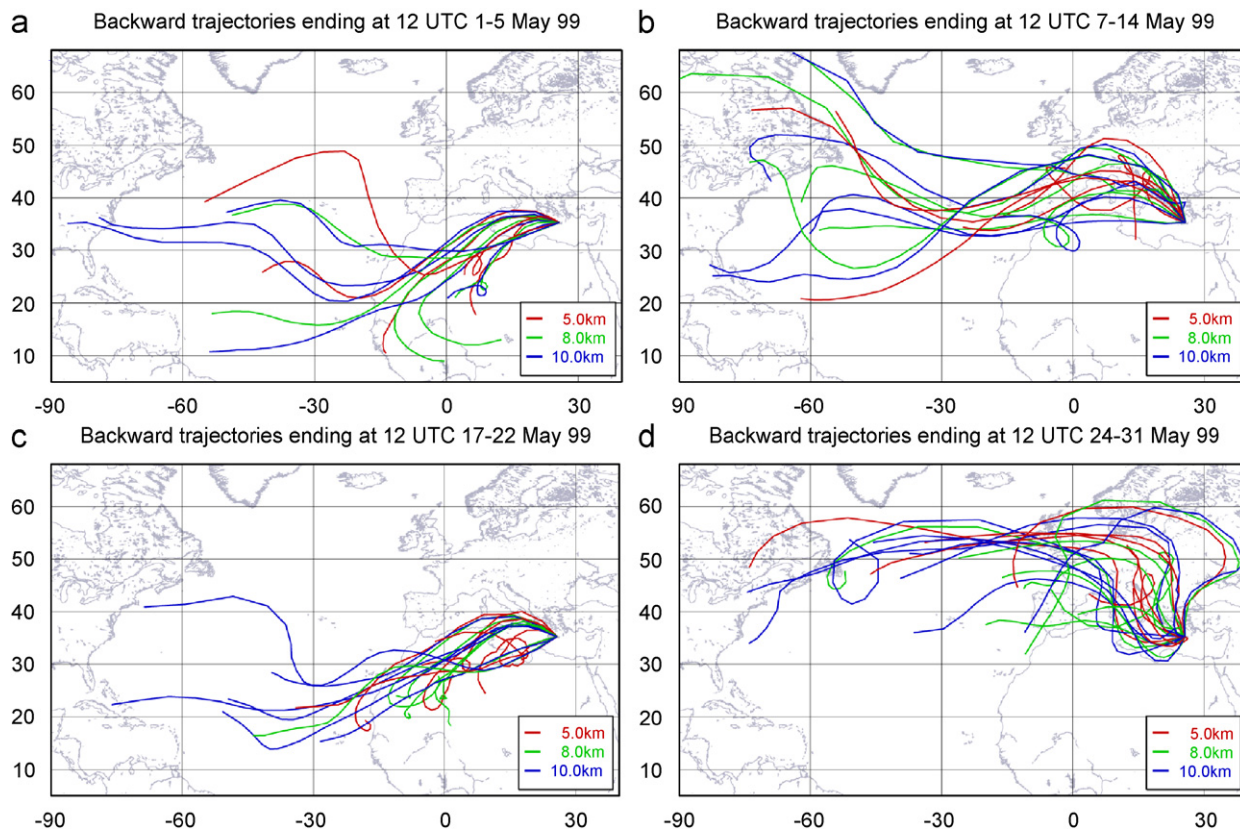


Fig. 2. (a) Five-day back-trajectories of air masses arriving at Finokalia in 1999 showing strong influence from the tropical upper troposphere (1–5 May), (b) the upper troposphere over industrialised regions in Europe (6–14 May), (c) Northern Africa free troposphere (15–23 May), and (d) NW Europe, the Balkans and the Black Sea free troposphere (24–31 May), calculated using Traj.x.

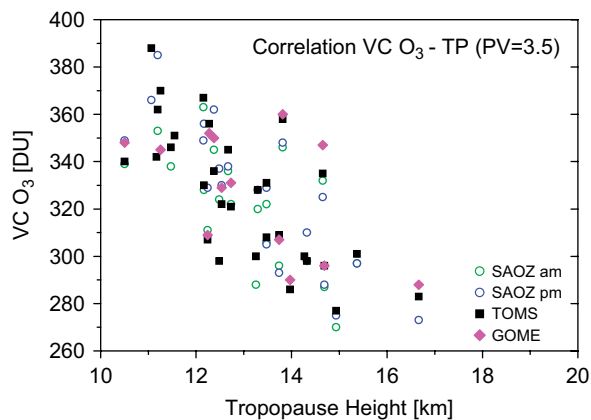


Fig. 3. Variability of  $VCD_{tot} O_3$  (DU) over Crete as a function of the tropopause height.

the applicability of the TEM to GOME data is investigated. In the extra-tropical regions, like the Mediterranean, the simplification that stratospheric

columns of  $O_3$  are approximately constant at a given latitude, shows limitations because the height of the tropopause can rapidly change within a day as the area oscillates between tropical and mid-latitude regimes. For each regime, the daily  $VCD_{tot} O_3$  remains constant with longitude and shows a clearly distinguishable behaviour (Hudson et al., 2003). For a successful calculation of  $O_3$  tropospheric columns with the TEM, the reference profile is required to be located in the same  $O_3$  regime as the profile to be analysed, i.e., with a comparable tropopause height. The tropopause height over Crete as compared to the reference sectors (Pacific and Atlantic) at the same latitude in May for the years 1998–2002, shows usually a difference of 2–3 km, but sometimes also of up to 7 km. Over Crete, the tropopause height is in the range of 11–13 km in most cases, whereas it lies between 14 and 15 km over the reference regions. Caused by these differences, an overestimation of  $VCD_{trop} O_3$  over Crete is expected. As a first approximation, this

overestimation is computed from sonde measurements (Thompson et al., 2003) to around 7 DU for May 1999. Consequently,  $VCD_{\text{trop}} \text{O}_3$  derived from GOME have to be considered with caution. Nevertheless, the synergistic use of GOME, TOMS, LIDAR and ozonesonde measurements is providing robust results (Fig. 4).

To derive the  $VCD_{\text{trop}} \text{O}_3$  from the ozonesondes, their profile data have been integrated up to 12-km height, equivalent to the tropopause height (derived from the criterion as described above) for the days on which sondes were launched. Ozone profiles from LIDAR measurements have been integrated up to 6 km (maximum height of observations) and extrapolated up to 12 km. The overall uncertainties in the  $VCD_{\text{trop}} \text{O}_3$  derived from sonde and LIDAR data (up to 6 km) are  $\pm 5\%$  and from the total LIDAR profile  $\pm 25\%$ . Due to the limited temporal and spatial overlap of GOME and LIDAR observations, the results of these instruments can be directly compared only on the 6th and 8th of May 1999 and differ by 15%. Ozonesonde measurements are available for 3 days (9–11 May 1999) with no direct coincidence with GOME overpasses over Crete. Direct comparisons of TOMS and GOME measurements show differences of around 30%. Based on the combined results of the four instruments, the  $VCD_{\text{trop}} \text{O}_3$  increased by 25 DU (from 27 to 52 DU) between 5th and 10th May and decreased afterwards, reaching background conditions of 20 DU on 22nd May. These results are in agreement with observations in the Mediterranean by Kourtidis et al. (2002). To determine if the variation in the

$VCD_{\text{trop}} \text{O}_3$  is mainly localised in the upper or lower troposphere, LIDAR and ozonesonde data were additionally integrated up to a height of 5 km. The results show an increase in of around 7 DU in the lower troposphere, that could be due to dynamical or photochemical buildup of  $\text{O}_3$  (Fig. 4). This enhancement is correlated to the increase of the total tropospheric amount. The remaining tropospheric  $\text{O}_3$  enhancement of 18 DU occurred in the upper troposphere. The ozonesonde profiles measured up to a height of 30–35 km show filaments of this trace gas in an atmospheric layer of 8–10-km height and an increase around 12 km, e.g., on 10 May 1999, indicating strong influence of stratospheric air masses at this altitude associated with the sub-tropical front during May 1999 (Fig. 5).

### 3.3. Buildup and transport of tropospheric trace gases over the Mediterranean region in May 1999

During May 1999, GOME measurements indicate that the  $VCD_{\text{tot}}$  and  $VCD_{\text{trop}} \text{O}_3$  loading is mainly influenced by the origin of the air masses arriving over Crete (Fig. 2). When air masses are not affected by Western European pollution (e.g., 1–5 May) or originate in Northern Africa (e.g., 15–23 May), like those prevailing in South wind regimes, anthropogenic influence on these air masses is negligible and tropospheric ozone levels over Crete remain low. In contrast, air masses being transported from industrial regions in Central Europe (e.g., 6–14 May) or from Western Europe, the Balkans and the Black Sea (24–31 May) towards Crete, are strongly influenced by anthropogenic emissions. The  $VCD_{\text{trop}}$  of  $\text{NO}_2$  and  $\text{HCHO}$

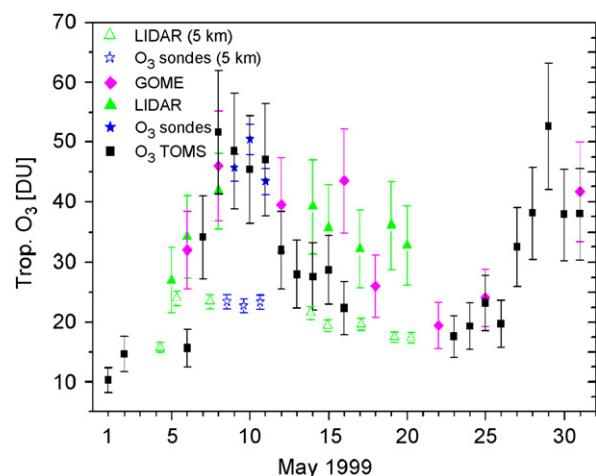


Fig. 4. Variation of  $VCD_{\text{trop}} \text{O}_3$  (DU) derived from GOME, ozonesondes, LIDAR and TOMS observations over Crete, in May 1999; tropospheric  $\text{O}_3$  column up to a height of 5 km.

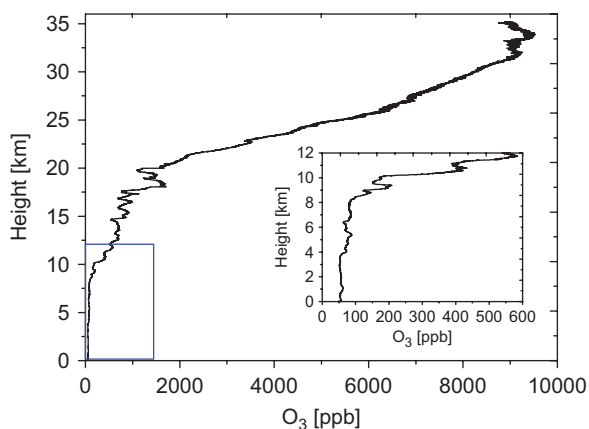


Fig. 5.  $\text{O}_3$  profile (ppb) from sonde measurements on 10 May 1999.

observed by the GOME instrument over Crete in an air mass that has passed over pollution sources are higher than the  $VCD_{\text{trop}}$  over the starting area of the trajectory a few days earlier when located over the relatively clean Atlantic Ocean. This difference in the  $VCD_{\text{trop}}$  over two different areas is mainly attributed to emissions and processing during transport. For instance, when an air mass originating from the West Atlantic Ocean (6th May) passed over West Europe before reaching Crete on 9th May, the observed  $VCD_{\text{trop}}$  over the starting point of the trajectory and over Crete, respectively, were for  $\text{NO}_2$   $0.8 \times 10^{15}$  and  $1.1 \times 10^{15}$  molecules  $\text{cm}^{-2}$  and for  $\text{HCHO}$   $1.1 \times 10^{16}$  and  $1.4 \times 10^{16}$  molecules  $\text{cm}^{-2}$ . Similarly, air masses originating from the East Atlantic (26 May) transported over Northern Europe and Balkans arrived over Crete on 31 May. The observed  $VCD_{\text{trop}}$  over East Atlantic and over Crete, respectively, were for  $\text{NO}_2$   $1.4 \times 10^{15}$  and  $1.8 \times 10^{15}$  molecules  $\text{cm}^{-2}$ , and for  $\text{HCHO}$   $1.6 \times 10^{16}$  and  $1.8 \times 10^{16}$  molecules  $\text{cm}^{-2}$ . However, when air masses are mainly influenced by South wind regimes, the tropospheric  $\text{NO}_2$  amounts over Crete are around  $5.0 \times 10^{14}$  molecules  $\text{cm}^{-2}$  and  $\text{HCHO}$  around  $2.5 \times 10^{15}$  molecules  $\text{cm}^{-2}$ .

The tropospheric  $\text{O}_3$  increase rates vary between 0.4 and  $0.9 \text{ DU h}^{-1}$ , as deduced from radiosonde measurements from Heraklion and LIDAR measurements carried out on Crete in May 1999. Similar results ( $0.4\text{--}2$  and  $0.3 \pm 0.1 \text{ DU h}^{-1}$ ) assuming a constant mixing ratio profile (from surface to the

tropopause at 12 km), are derived from surface hourly observations at Finokalia (Kouvarakis et al., 2002; Gerasopoulos et al., 2006). During the PAUR experiment, Zanis et al. (2002) evaluated a morning net  $\text{O}_3$  production rate of  $0.8\text{--}1.3 \text{ ppbv h}^{-1}$  corresponding to a column increase of  $0.5\text{--}0.9 \text{ DU h}^{-1}$ . Taking into account a 12-h photochemical activity per day over the area during May, the LIDAR observations suggest a dynamical and/or photochemical buildup of  $6.3\text{--}10.5 \text{ DU day}^{-1}$  (based on the mean value of  $0.7 \text{ DU h}^{-1}$ ) of tropospheric  $\text{O}_3$ , including the associated uncertainties.

The involvement of STE in the observed ozone increase has been also investigated. Fig. 6(a) shows the monthly mean fraction of back-trajectories influenced by the stratosphere and arriving over Crete in May 1999. Up to about 30% (of the considered air parcels in the altitude range between 10 and 12 km) are influenced by the stratosphere. These results are subject to back-trajectory calculation uncertainties and applicability to satellite observations (Stohl et al., 2002). When considering the transport of  $\text{O}_3$  into the troposphere (according to the methodology described in Section 2.3), a tropospheric  $\text{O}_3$  amount of about 10 DU originates from the stratosphere. Peak values of up to 20 DU (26 May 1999) can be seen in the time series of STE-ozone in the vicinity of Crete for May 1999 (Fig. 6(b)).

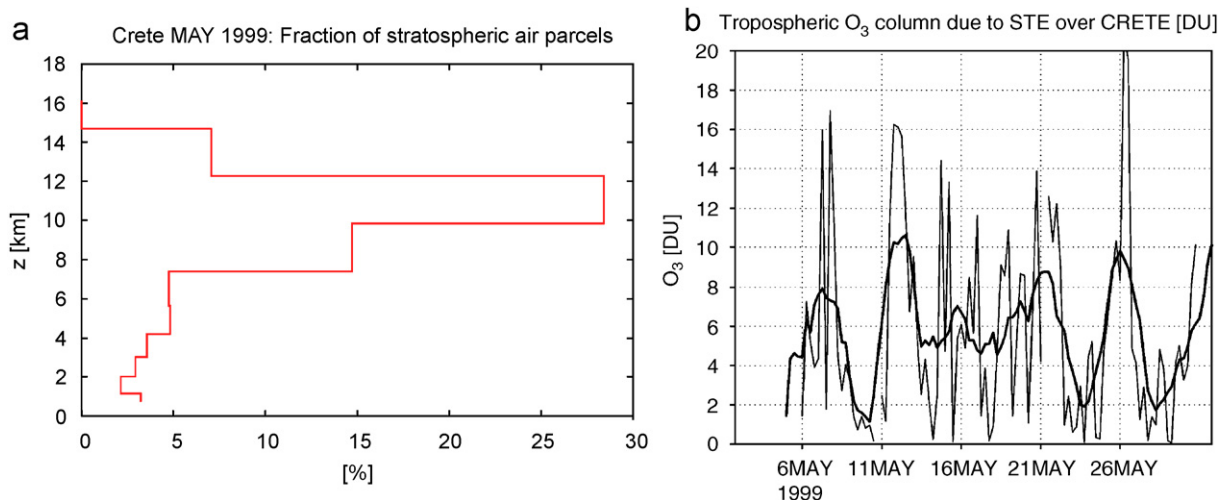


Fig. 6. ROSE model results: (a) altitude-dependent monthly mean fraction of stratospheric influenced trajectories (%) arriving in the troposphere over Crete, (b) timeseries of  $VCD_{\text{trop}} \text{O}_3$  (DU) due to STE over Crete in May 1999 (thin line indicates the 6-hourly mean and the thick line a 2-day-running-mean of the STE-ozone column density).

### 3.4. Seasonality and inter-annual variation in spring

The representativeness of the May 1999 study presented here is investigated by studying the inter-annual trends and seasonal variations of tropospheric  $O_3$  precursors over Crete. For the years 1996–2002, the monthly mean  $VCD_{trop}$  are in the range of  $1.5 \times 10^{14}$ – $1.6 \times 10^{15}$  molecules  $cm^{-2}$  for  $NO_2$  (lowest in March and highest in July) and  $4.1 \times 10^{14}$ – $8.3 \times 10^{15}$  molecules  $cm^{-2}$  for HCHO (lowest in December and highest in July) (Fig. 7a and b). Comparing the winter (DJF) and summer (JJA) seasons, an increase of  $4.1 \times 10^{14}$  molecules  $cm^{-2}$  is deduced for  $NO_2$  tropospheric columns and of  $4.2 \times 10^{15}$  molecules  $cm^{-2}$  for HCHO  $VCD_{trop}$ . Similar seasonality (agreement within 10%,  $r^2 = 0.53$ ) deduced from ground-based  $NO_2$  observations in

2002 (Vrekoussis et al., 2007) (Fig. 7a). The magnitudes of the seasonal variations of both  $NO_2$  and HCHO  $VCD_{trop}$  are twice the uncertainties of the retrievals. This significant increase in HCHO  $VCD_{trop}$  can be attributed to VOCs from biogenic, anthropogenic and biomass burning sources.

Focussing on May, no clear inter-annual trend is observed from 1996 to 2002. The monthly mean of  $NO_2$  and HCHO  $VCD_{trop}$  from GOME equal  $1.1 \times 10^{15}$  and  $4.7 \times 10^{15}$  molecules  $cm^{-2}$ , respectively. These columns correspond to boundary layer mixing ratios of 0.4 ppb  $NO_2$  and 1.5 ppb HCHO (assuming a boundary layer height of 1.3 km) in reasonable agreement with observations of  $NO_2$  ( $0.42 \pm 0.49$  ppb) (Vrekoussis et al., 2006, 2007) and of HCHO under ‘unpolluted’ conditions at Heraklion, Crete, in 2002 ( $\sim 1$  ppb) (Mihalopoulos N., personal communication).

Additionally, the composite distributions of  $NO_2$  and HCHO over Greece were determined for GOME from May 1996 to 2002 (Fig. 8a and b). Background conditions for  $NO_2$  and HCHO over Crete ( $1.1 \times 10^{15}$  and  $4.7 \times 10^{15}$  molecules  $cm^{-2}$ , respectively) and enhancements of  $NO_2$  due to pollution over the urban areas of Athens and Thessaloniki as well as Istanbul can be observed. Tropospheric amounts of  $NO_2$  and HCHO from GOME for background conditions for Crete, clean-air Atlantic ocean and polluted air regions upwind Crete for May, averaged over 1996–2002 are listed in Table 1. The  $NO_2$  and HCHO  $VCD_{trop}$  are a factor of about 2 and 1.5, respectively, higher over Crete than over the Atlantic. To distinguish between natural and anthropogenic influences, the ratio of HCHO/ $NO_2$  is calculated from GOME data. The lowest values (1.5–2.6) of this ratio are determined over the most polluted upwind regions (the Po-Valley, Istanbul, Thessaloniki and Athens) due to fresh emissions of  $NO_x$  and not sufficient breakdown of emitted VOCs to form HCHO. The ratio increases towards Crete to a value of 4.3. This could indicate that during the transport, the short-lived  $NO_2$  is converted to  $HNO_3$  (Vrekoussis et al., 2006) and the air masses are potentially enriched in HCHO from regional sources affecting this marine location (Liakakou et al., 2007). Additionally, based on the chemical box model (Section 2.2), the photochemical production of  $O_3$  associated with the observed  $NO_2$  and HCHO  $VCD_{trop}$  under the conditions prevailing over Crete, for a day of 12 h was calculated (Table 1). The results underline that  $P_{O_3}$  over urban polluted regions is higher

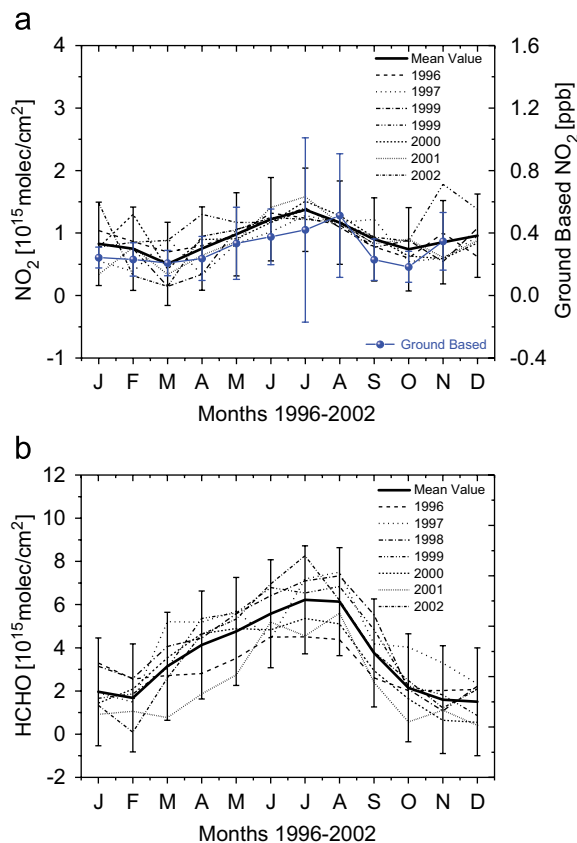


Fig. 7. (a) Monthly averages over Crete for  $VCD_{trop}$   $NO_2$  for 1996–2002 molecules  $cm^{-2}$ ; including retrieval errors for the mean value of  $6 \times 10^{14}$  molecules  $cm^{-2}$  (left axis) and boundary layer  $NO_2$  observations for 2002 ppb including retrieval errors; (right axis, blue coloured), and (b) monthly averages of  $VCD_{trop}$  HCHO columns from GOME for 1996–2002 (molecules  $cm^{-2}$ ) including retrieval errors for the mean value of  $2.5 \times 10^{15}$  molecules  $cm^{-2}$ .

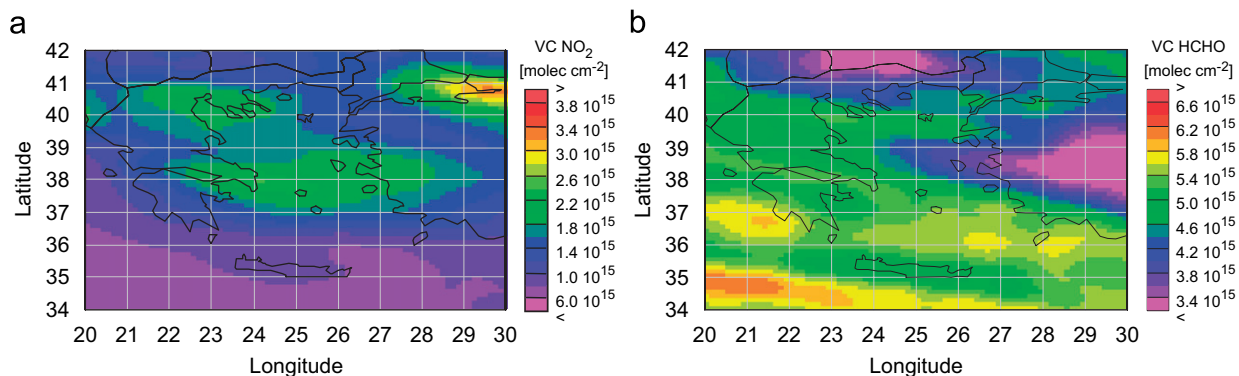


Fig. 8. Monthly composites of tropospheric  $\text{NO}_2$  (a) and HCHO columns (b) ( $\text{molecules cm}^{-2}$ ) for May 1996–2002 from GOME.

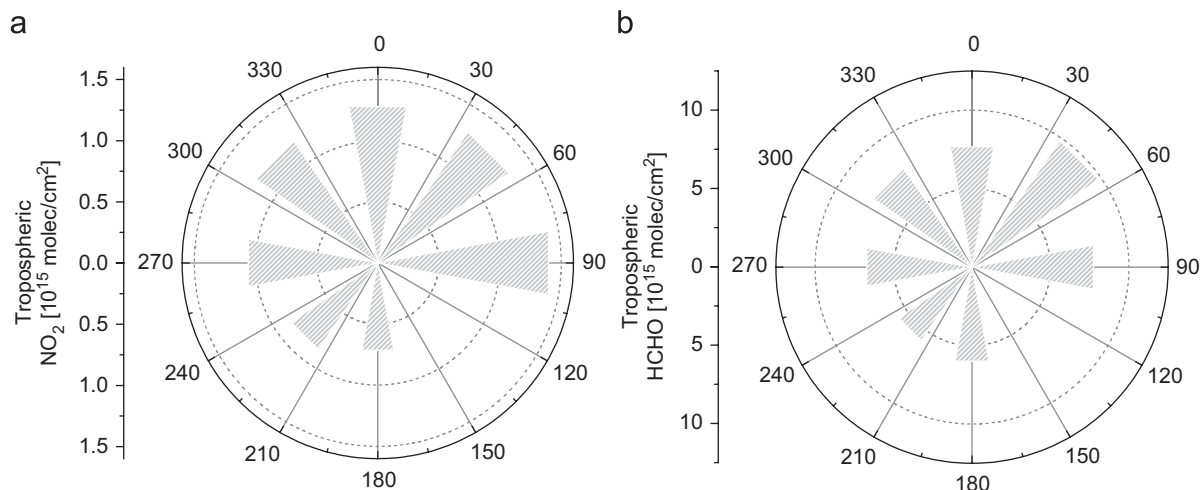


Fig. 9.  $\text{VCD}_{\text{trop}}$   $\text{NO}_2$  (a) and HCHO (b) ( $\text{molecules cm}^{-2}$ ) for 1996–2002 from GOME as function of wind sector as determined from the back-trajectories.

(1.1–2.1  $\text{DU day}^{-1}$ ) compared to clean-air regions Atlantic and Crete ( $\leq 1.0 \text{ DU day}^{-1}$ ). Similar results are also obtained when including other VOCs besides HCHO in this calculation ( $P_{\text{O}_3\text{-VOC}}$ ). This is done as a sensitivity test by assuming 10 times higher HCHO or, only for Crete, by using real observed VOC background concentrations. The deduced  $P_{\text{O}_3\text{-VOC}}$  has to be considered as the order of magnitude of the VOC impact on tropospheric chemistry since global models (Myriokefalitakis, 2006; Wittrock et al., 2006) estimate a VOC to HCHO concentration ratio over the continents surrounding the Mediterranean between 4 and 10. As can be seen from Table 1, Crete is mainly influenced by clean-air conditions and therefore the local production of tropospheric  $\text{O}_3$  is expected to

be negligible in May. Nevertheless, polluted air masses are occasionally transported to this region. The dependency of the tropospheric amounts of  $\text{NO}_2$  and HCHO on wind direction from 1996 to 2002 deduced from GOME is shown in Fig. 9a and b. These figures reinforce the results for 1999, showing higher  $\text{NO}_2$  and HCHO  $\text{VCD}_{\text{trop}}$  (by 1.1 and 1.2 times, respectively) when Crete is influenced by air masses from Europe and the Balkan (NW–N–NE) compared to those observed when air masses are coming from the West. Similar results are observed when comparing the NW–N–NE and SW–S sectors (factor of 1.6 for  $\text{NO}_2$  and of 1.4 for HCHO). Therefore, except for these described sporadic meteorological conditions, Crete can be considered as an unpolluted area.

#### 4. Conclusions

The synergistic use of GOME data with back-trajectory analysis and box model calculations enabled the detection of significant changes in pollutant tropospheric columns related to general air circulation patterns. When the Mediterranean is influenced by air masses from Central Europe, the Balkans and the Black Sea, pollution leads to an increase in  $\text{NO}_2$  and  $\text{HCHO VCD}_{\text{trop}}$  and, consequently,  $\text{VCD}_{\text{trop O}_3}$ . From the observed  $\text{VCD}_{\text{trop O}_3}$  increase of about 25 DU, only about  $1 \text{ DU day}^{-1}$  can be attributed to local and  $2\text{--}8 \text{ DU day}^{-1}$  to regional  $\text{O}_3$  photochemical buildup within upwind polluted air masses and about 10 DU (peaking up to 20 DU) in maximum to STE, depending on the meteorological situation. The remaining part (up to 13 DU) is to be attributed to long-range transport of  $\text{O}_3$  from polluted regions. Urban areas upwind Crete like Athens, Thessaloniki, Istanbul and the Po Valley can be seen from GOME as pollution sources. Thus, when air masses are reaching Crete from the NW–N–NE wind sector, passing over these areas, an increase in the tropospheric amounts of  $\text{NO}_2$  and  $\text{HCHO}$  is observed by GOME compared to situations with air masses originating from the SW–S sector.

The analysis of GOME data for the 7-year period (1996–2002) shows no significant year-to-year change in the tropospheric amounts of  $\text{NO}_2$  and  $\text{HCHO}$  and consequently in the production of tropospheric  $\text{O}_3$  in May. The observed seasonal variation of the  $\text{NO}_2$  and  $\text{HCHO VCD}_{\text{trop}}$  indicates higher values during the warm period of intensive photochemistry attributed to long-range transport of  $\text{NO}_x$  from upwind pollution sources and also increased biogenic emissions of VOC. The monthly mean  $\text{VCD}_{\text{trop}}$  of both  $\text{NO}_2$  and  $\text{HCHO}$  are 1.6–3.5 and 1.1–1.4 times less than over upwind pollution regions and can be considered as background conditions for the East Mediterranean.

#### Acknowledgements

This study has been initiated and supported by a German–Greek bilateral collaboration project. In addition, this work has been funded by the Universities of Bremen and Crete and facilitated by the EU Network of excellence ACCENT. We thank Prof. C. Zerefos for PAUR data, Prof. A. M. Thompson for ozone sonde data, M. Weber for  $\text{O}_3$

from GOME, Prof. N. Mihalopoulos for fruitful discussion, G. Tzirita for data manipulation and R.B.A. Koelemeijer for the FRESCO data. M. Vrekoussis acknowledges Alexander von Humboldt Foundation post-doctoral fellowship. E. Dermitzaki acknowledges support by a PENED grant 03ED-169, co-funded by the Greek Ministry of Development and the European Social Fund.

#### References

- Atkinson, R., Baulch, D.L., Cox, R.A., Crowley, J.N., Hampson, R.F., Hynes, R.G., Jenkin, M.E., Rossi, M.J., Troe, J., 2004. Evaluated kinetic and photochemical data for atmospheric chemistry: volume I—gas phase reactions of  $\text{O}_x$ ,  $\text{HO}_x$ ,  $\text{NO}_x$  and  $\text{SO}_x$  species. *Atmospheric Chemistry and Physics* 4, 1461–1738.
- Atkinson, R., Baulch, D.L., Cox, R.A., Crowley, J.N., Hampson, R.F., Hynes, R.G., Jenkin, M.E., Rossi, M.J., Troe, J., 2006. Evaluated kinetic and photochemical data for atmospheric chemistry: volume II—reactions of organic species. *Atmospheric Chemistry and Physics* 6, 3625–4055.
- Baier, F., Erbertseder, T., Morgenstern, O., Bittner, M., Brasseur, G., 2005. Assimilation of MIPAS observations using a three-dimensional global chemical-transport model. *Quarterly Journal of the Royal Meteorological Society* 131 (613–Part c), 3529–3542.
- Boersma, K.F., Eskes, H.J., Brinksma, E.J., 2004. Error analysis for tropospheric  $\text{NO}_2$  retrieval from space. *Journal of Geophysical Research* 109, D04311.
- Burrows, J.P., et al., 1999. The Global Ozone Monitoring Experiment (GOME): mission concept and first scientific results. *Journal of Atmospheric Sciences* 56, 151–175.
- Calpini B., et al., 1997. Ozone LIDAR as an analytical tool in effective air pollution management. In: *The Geneva 96 Campaign Chimia*, no. 51, pp. 700–704.
- Chance, K., Palmer, P., Spurr, R.J.D., Martin, R.V., Kurosu, T.P., Jacob, D.J., 2000. Satellite observations of formaldehyde over North America from GOME. *Geophysical Research Letters* 27, 3461–3464.
- Coldewey-Egbers, M., Weber, M., Lamsal, L.N., de Beek, R., Buchwitz, M., Burrows, J.P., 2005. Total ozone retrieval from GOME UV spectral data using the weighting function DOAS approach. *Atmospheric Chemistry and Physics* 5, 5015–5025.
- Fishman, J., Crutzen, P.J., 1978. The origin of ozone in the troposphere. *Nature* 274, 855–858.
- Fishman, J., Watson, C.E., Larsen, J.C., Logan, J.A., 1990. Distribution of tropospheric ozone determined from satellite data. *Journal of Geophysical Research* 95, 3599–3617.
- Gerasopoulos, E., Kouvarakis, G., Vrekoussis, M., Donoussis, Ch., Mihalopoulos, N., Kanakidou, M., 2006. Photochemical ozone production in the Eastern Mediterranean. *Atmospheric Environment* 40, 3057–3069.
- Goutail, F., Pommereau, J.P., 1991. Comparison of ground-based SAOZ and satellite TOMS total ozone observations at polar latitudes. In: *Proceedings of the First European Workshop on Polar Stratospheric Ozone Research*, ECC Editor.

- Goutail, F., et al., 1999. Depletion of column ozone in the Arctic during the winters of 1993–94 and 1994–95. *Journal of Atmospheric Chemistry* 32, 1–34.
- Hudson, R.D., Thompson, A.M., 1998. Tropical tropospheric ozone from total ozone mapping spectrometer by a modified residual method. *Journal of Geophysical Research* 103, 22129–22145.
- Hudson, R.D., Frolov, A.D., rade, M.F., Follette, M.B., 2003. The total ozone field separated into meteorological regimes. Part I: defining the regimes. *Journal of Atmospheric Sciences* 60 (14), 1669–1677.
- Koelemeijer, R.B.A., Stammes, P., Hovenier, J.W., de Haan, J.F., 2001. A fast method for retrieval of cloud parameters using oxygen A—band measurements from GOME. *Journal of Geophysical Research* 106, 3475–3490.
- Kourtidis, K., Zerefos, C., Rapsomanikis, S., Simeonov, V., Balis, D., Perros, P.E., Thompson, A.M., Witte, J., Calpini, B., Sharobim, W.M., Papayannis, A., Mihalopoulos, N., Drakou, R., 2002. Regional levels of ozone in the troposphere over eastern Mediterranean. *Journal of Geophysical Research* 107, 18, 8140.
- Kouvarakis, G., Vrekoussis, M., Mihalopoulos, N., Kourtidis, K., Rappengluck, B., Gelasopoulos, E., Zerefos, C., 2002. Spatial and temporal variability of tropospheric ozone ( $O_3$ ) in the boundary layer above the Aegean Sea Eastern Mediterranean. *Journal of Geophysical Research* 107, 8137.
- Ladstätter-Weissenmayer, A., Burrows, J.P., Perner, D., 1998. Biomass burning over Indonesia as observed by GOME. *Earth Observation Quarterly* 58, 28–30.
- Ladstätter-Weissenmayer, A., Heland, J., Kormann, R., v. Kuhlmann, R., Lawrence, M.G., Meyer-Arnek, J., Richter, A., Wittrock, F., Ziereis, H., Burrows, J.P., 2003. Transport and build-up of tropospheric trace gases during the MINOS campaign: comparison of GOME, in situ aircraft measurements and MATCH-MPIC-data. *Atmospheric Chemistry and Physics* 3, 1887–1902.
- Ladstätter-Weissenmayer, A., Meyer-Arnek, J., Schlemm, A., Burrows, J.P., 2004. Influence of stratospheric air masses on tropospheric vertical  $O_3$  columns based on GOME (Global Ozone Monitoring Experiment) measurements and back-trajectory calculation over the Pacific. *Atmospheric Chemistry and Physics* 4, 903–909.
- Lawrence, M.G., Butler, T.M., Steinkamp, J., Gurjar, B.R., Lelieveld, J., 2006. Regional pollution potentials of megacities and other major population centers. *Atmospheric Chemistry and Physics Discussion* 6, 13323–13366.
- Leue, C., Wenig, M., Wagner, T., Klimm, O., Platt, U., Jähne, B., 2001. Quantitative analysis of  $NO_x$  emissions from GOME satellite image sequences. *Journal of Geophysical Research* 106, 5493–5505.
- Liakakou, E., Vrekoussis, M., Bonsang, B., Donousis, Ch., Kanakidou, M., Mihalopoulos, N., 2007. Isoprene above the Eastern Mediterranean: seasonal variation and contribution to the oxidation capacity of the atmosphere. *Atmospheric Environment* <doi:10.1016/j.atmosenv.2006.09.034>.
- Martin, R.V., Chance, K., et al., 2002. An improved retrieval of tropospheric nitrogen dioxide from GOME. *Journal of Geophysical Research* 107, 20.
- McPeters, R.E.A., 1996. Nimbus-7 Total Ozone Mapping Spectrometer (TOMS) Data Products User's Guide. NASA Ref. Publ., p. 1384.
- Meyer-Arnek, J., Ladstätter-Weissenmayer, A., Richter, A., Wittrock, F., Burrows, J.P., 2005. A study of the trace gas columns of  $O_3$ ,  $NO_2$  and HCHO over Africa in September 1997. *Faraday Discussion* 130, 387.
- Myriokefalitakis S., 2006. Development of chemical code and application for the study of the global distribution of Glyoxal and Formaldehyde with the use of the three-dimensional chemical transport model TM4. Master Thesis, University of Crete, Greece.
- Oltmans, S.J., Lefohn, A.S., et al., 1998. Trends of ozone in the troposphere. *Geophysical Research Letters* 25, 139.
- Palmer, P.I., Jacob, D.J., Fiore, A.M., Martin, R.V., Chance, K., Kurosu, T.P., 2002. Mapping isoprene emissions over North America using formaldehyde columns observations from space. *Journal of Geophysical Research* 101, 2053–2072.
- Poisson, N., Kanakidou, M., et al., 2001. The impact of natural non methane hydrocarbon oxidation on the free radical and ozone budgets above a eucalyptus forest. *Chemosphere, Global Change Science* 3, 353–366.
- Randriambelo, T., Baray, J.L., Baldy, S., Bremaud, P., Cautenet, S., 1999. A case study of extreme tropospheric ozone contamination in the tropics using in-situ, satellite and meteorological data. *Geophysical Research Letters* 26, 1287–1290.
- Richter, A., Burrows, J.P., 2002. Retrieval of tropospheric  $NO_2$  from GOME measurements. *Advanced Space Research* 29 (11), 1673–1683.
- Rose, K., Brasseur, G., 1989. A three-dimensional model of chemically active trace species in the middle atmosphere during disturbed winter conditions. *Journal of Geophysical Research* 94, 16 387–16 403.
- Rozanov, V., Diebel, D., Spurr, R.J.D., Burrows, J.P., 1997. GOMETRAN: a radiative transfer model for the satellite project GOME—the plane parallel version. *Journal of Geophysical Research* 10214. 16 683–16 695, <doi:10.1029/96JD01535>.
- Simeonov, V., et al., 1998. The EPFL UV Ozone DIAL: results and upgrades, In: NASA editor, Proceedings of the 19th ILRC, pp. 399–402.
- Stohl, A., Eckhardt, S., Forstera, C., James, P., Spichtingera, N., Seibert, P., 2002. A replacement for simple back trajectory calculations in the interpretation of atmospheric trace substance measurements. *Atmospheric Environment* 36, 4635–4648.
- Thompson, A.M., et al., 2003. Southern hemisphere additional ozonesondes (SHADOZ) 1998–2000 tropical ozone climatology—1. Comparison with total ozone mapping spectrometer (TOMS) and ground-based measurements. *Journal of Geophysical Research* 108 (D2), 8238.
- Tsigaridis, K., Kanakidou, M., 2002. Importance of volatile organic compounds photochemistry over a forested area in Central Greece. *Atmospheric Environment* 36 (19), 3137–3146.
- Vrekoussis, M., Kanakidou, M., et al., 2004. Role of the  $NO_3$  radicals in oxidation processes in the eastern Mediterranean troposphere during the MINOS campaign. *Atmospheric Chemistry and Physics* 4, 169–182.
- Vrekoussis, M., Liakakou, E., Mihalopoulos, N., Kanakidou, M., Ctutzen, P.J., Lelieveld, J., 2006. Formation of  $HNO_3$  and  $NO_3^-$  in the anthropogenically-influenced eastern Mediterranean marine boundary layer. *Geophysical Research Letters* 33, L05811.

- Vrekoussis, M., Mihalopoulos, N., Gerasopoulos, E., Kanakidou, M., Crutzen, P.J., Lelieveld, J., 2007. Two-years of NO<sub>3</sub> radical observations in the boundary layer over the Eastern Mediterranean. *Atmospheric Chemistry and Physics* 7, 315–327.
- Waugh, D.W., Polvani, L.M., 2000. Climatology of intrusions into the tropical upper troposphere. *Geophysical Research Letters* 27, 3857–3860.
- Wayne, R., 2000. *Chemistry of Atmospheres*, Oxford University Press, third ed.
- Weber, M., Lamsal, L.N., Coldewey-Egbers, M., Bramstedt, K., Burrows, J.P., 2005. Pole-to-pole validation of GOME WFDAS total ozone with groundbased data. *Atmospheric Chemistry and Physics* 5 (9289), 1341–1355.
- Wittrock, F., Richter, A., et al., 2006. Simultaneous global observations of glyoxal and formaldehyde from space. *Geophysical Research Letters* 33, L16804.
- Zanis, P., Kourtidis, K., et al., 2002. A case study on the possible link between surface ozone photochemistry and total ozone column during the PAUR II experiment at Crete: comparison of observations with box model calculations. *Journal of Geophysical Research Atmosphere* 107D18.
- Zerefos, C.S., et al., 2002. Photochemical activity and solar ultraviolet radiation modulation factors (PAUR): an overview of the project. *Journal of Geophysical Research* 107DX, <doi:10.1029/2000JD000134>.